

Low field magnetotransport properties of $(\text{La}_{0.7}\text{Sr}_{0.3}\text{MnO}_3)_{0.5}:(\text{ZnO})_{0.5}$ nanocomposite films

B. S. Kang,^{a),b)} H. Wang, J. L. MacManus-Driscoll,^{c)} Y. Li, and Q. X. Jia^{a),d)}
Superconductivity Technology Center, Los Alamos National Laboratory, Los Alamos, New Mexico 87545

I. Mihut and J. B. Betts
National High Magnetic Field Laboratory, Los Alamos National Laboratory, Los Alamos, New Mexico 87545

(Received 29 November 2005; accepted 11 March 2006; published online 11 May 2006)

$(\text{La}_{0.7}\text{Sr}_{0.3}\text{MnO}_3)_{0.5}:(\text{ZnO})_{0.5}$ nanocomposite thin films were deposited on *c*-cut sapphire substrates via pulsed laser deposition. The as-grown films were composed of fine grains of 20–50 nm size. The epitaxial orientation relationships between the $\text{La}_{0.7}\text{Sr}_{0.3}\text{MnO}_3$ (LSMO) and the sapphire was $(111)_{\text{LSMO}}//\langle 0003 \rangle_{\text{Al}_2\text{O}_3}$ and $\langle 11\bar{2} \rangle_{\text{LSMO}}//\langle 10\bar{1}0 \rangle_{\text{Al}_2\text{O}_3}$. A low field magnetoresistance (LFMR) of $\sim 12\%$ was achieved at an external magnetic field of $H=1$ T at 77 K, possibly due to enhanced grain boundary effects. The postannealed film had columnar structures with well-crystallized large grains (~ 200 nm), and showed a low resistivity and consequently negligible LFMR similar to that of single crystal LSMO. © 2006 American Institute of Physics. [DOI: 10.1063/1.2197317]

The discovery of colossal magnetoresistance (CMR) in rare-earth manganites of $R_{1-x}A_x\text{MnO}_3$ (where *R* is rare earth and *A* is divalent cation) has triggered enormous studies on these perovskite-based materials over the last decade.^{1,2} However, the intrinsic CMR effect in the perovskite manganites is observed only under high magnetic fields of several teslas at a narrow range of temperatures around the ferromagnetic-paramagnetic phase transition, which has greatly limited its practical applications. Therefore, it is highly desirable to exploit low field magnetoresistance (LFMR) that can be triggered at an external magnetic field of the order of the coercive field H_c .

Improvements of LFMR have been achieved either by making the manganites in polycrystalline granular structure^{2–5} or by incorporating other materials to enhance the spin-polarized tunneling through grain boundaries.^{6–10} Through various secondary phase attempts using insulators,^{6–8} glass,⁹ and other CMR oxides¹⁰ to make polycrystalline films, many researchers have sacrificed crystallinity and epitaxial orientation to obtain more grain boundaries. However, it is hard to achieve uniform properties in randomly oriented polycrystalline films with grain size of 0.2–2 μm .^{7,10} The importance of growing well-oriented manganite composites has been emphasized in a recent report on epitaxial $(\text{La}_{0.7}\text{Ca}_{0.3}\text{MnO}_3)_{1-x}:(\text{MgO})_x$ nanocomposite films.¹¹ It is, therefore, highly desirable to extend these composite approaches to various fields to acquire physical properties superior to those of naturally existing material systems.

In this letter, we report our successful growth of $(\text{La}_{0.7}\text{Sr}_{0.3}\text{MnO}_3)_{0.5}:(\text{ZnO})_{0.5}$ nanocomposite thin films and their magnetotransport properties. Since the ionic radius of Zn is rather different from that of La, Sr, or Mn, the Zn substitution for these ions is minimized. Therefore, we can avoid unexpected alterations in the spin-polarized nature of

$\text{La}_{0.7}\text{Sr}_{0.3}\text{MnO}_3$ (LSMO) that depends on the balance of La^{3+} and Sr^{2+} cations as well as Mn–O–Mn coupling. We demonstrate that as-grown films made by pulsed laser deposition (PLD) have a well-oriented structure with fine grains, while films postannealed at 1000 °C have a columnar structure with well-crystallized large grains. We compare the resistivity and LFMR properties of the films.

The LSMO:ZnO thin films were deposited on *c*-cut sapphire substrates by PLD using a XeCl excimer laser ($\lambda=308$ nm) operating at a repetition rate of 5 Hz. A substrate temperature of 750 °C and oxygen pressure of 200 mTorr were used during the deposition. After the deposition, the films were cooled in an oxygen atmosphere of 200 Torr. The postannealing was performed using a conventional furnace at 1000 °C for 1 h in an oxygen atmosphere.

Figure 1(a) shows the x-ray diffraction (XRD) θ - 2θ scans for the as-grown film and the postannealed film. The LSMO(111) orientation was predominant in both films. Figure 1(b) shows the XRD ϕ scans for the postannealed film. The ϕ -scan patterns of the as-grown film (not shown) were similar to those of the postannealed film except that the full width at half maximum (FWHM) values were larger, as shown in Table I. A clear threefold symmetry of LSMO(100) planes aligned to the sapphire $(10\bar{1}4)$ planes in the ϕ scan indicates that the majority grains of LSMO were grown in epitaxial relationships of $(111)_{\text{LSMO}}//\langle 0006 \rangle_{\text{Al}_2\text{O}_3}$ and $\langle 11\bar{2} \rangle_{\text{LSMO}}//\langle 10\bar{1}0 \rangle_{\text{Al}_2\text{O}_3}$. The result is remarkable since there has not been any report of successful growth of epitaxial LSMO thin films directly on *c*-cut sapphire substrates. A randomly textured $\text{La}_{0.67}\text{Sr}_{0.33}\text{MnO}_3$ film was reported from the growth on a *c*-cut sapphire by metal-organic chemical vapor deposition.¹² $\text{La}_{0.71}\text{Sr}_{0.29}\text{Mn}_{1.01}\text{O}_{3-\delta}$ films on $(11\bar{2}0)$ sapphire by sputtering also resulted in a mixed orientation of LSMO(001) and (011).¹³

Furthermore, ZnO(0002) peaks were observed in a threefold symmetry in the XRD ϕ -scan with the same ϕ and χ angles as those of the LSMO(110) poles [$\chi=\cos^{-1}(1/3^{1/2})\approx 54.7^\circ$], although no ZnO peak was observed in θ - 2θ scan. Since the *d* spacings of LSMO(110) and ZnO(0002) are close, we performed an XRD θ - 2θ scan with

^{a)} Authors to whom correspondence should be addressed.

^{b)} Electronic mail: bskang@lanl.gov

^{c)} Also at Department of Materials Science and Metallurgy, University of Cambridge, Cambridge CB2 3QZ, UK.

^{d)} Electronic mail: qxjia@lanl.gov

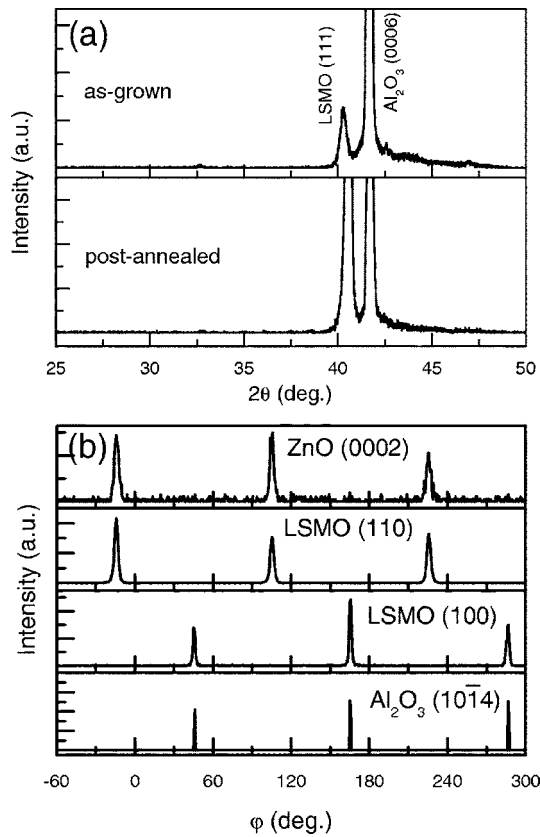


FIG. 1. X-ray diffraction (a) θ - 2θ scans and (b) ϕ scans for the as-grown films and the postannealed films.

$\chi=54.7^\circ$, where we observed two clearly separated peaks for the two planes. This shows that the majority grains of ZnO were grown in a unique pattern with their (000 l) planes parallel to the LSMO(110) planes.

To characterize the microstructures of the films before and after annealing, cross-sectional transmission electron microscopy (TEM) analysis was performed. Figure 2(a) shows a bright field low magnification TEM image of the as-grown film on a sapphire substrate. The grains are small and elongated along the c axis. The average grain size is in the range of 20–50 nm, which is smaller than other reported values for the as-grown composite manganite films with different additions.^{7–10} A corresponding selected-area diffraction (SAD) was carried out and is shown as an insert in Fig. 2(a). It is clear that both ZnO and LSMO have preferred orientations on sapphire. The orientation relations are determined to be $\langle 11\bar{2} \rangle_{\text{LSMO}} // \langle 0001 \rangle_{\text{ZnO}} // \langle 10\bar{1}0 \rangle_{\text{Al}_2\text{O}_3}$, $(111)_{\text{LSMO}} // (0003)_{\text{Al}_2\text{O}_3}$, and $(10\bar{1}0)_{\text{ZnO}} // (2\bar{1}\bar{1}0)_{\text{Al}_2\text{O}_3}$ (marked in SAD). This confirms the result of XRD on the orientation of LSMO, although the ZnO here is different from the majority grains observed in XRD. After annealing, the film has much bigger grains epitaxially grown on the sapphire substrate. More interestingly, high quality epitaxial

TABLE I. FWHM of the ϕ -scan peaks of the films.

Peaks	FWHM (deg) (As grown)	FWHM (deg) (Postannealed)
ZnO(0002)	5.6	2.1
LSMO(110)	6.5	3.4
LSMO(100)	7.2	3.8

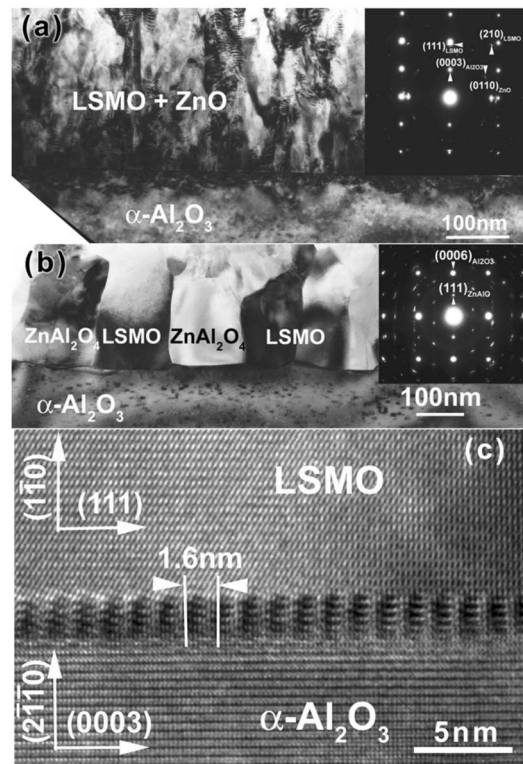


FIG. 2. Cross-sectional bright field low magnification TEM images of LSMO:ZnO on sapphire (a) before annealing and (b) after annealing. The corresponding SAD patterns are shown as inserts. (c) High resolution TEM image of the interface between LSMO and α - Al_2O_3 .

LSMO and ZnAl_2O_4 (a spinel phase due to the reaction of ZnO and Al_2O_3) have produced big alternating grains on sapphire as shown in Fig. 2(b). The average grain size was about 200 nm. SAD from the same area is shown as an insert in Fig. 2(b). The orientation relations have changed to $\langle 11\bar{2} \rangle_{\text{LSMO}} // \langle 011 \rangle_{\text{ZnAl}_2\text{O}_4} // \langle 10\bar{1}0 \rangle_{\text{Al}_2\text{O}_3}$ and $(001)_{\text{LSMO}} // (0003)_{\text{Al}_2\text{O}_3}$. Disregarding the case that ZnAl_2O_4 grains were grown epitaxially on sapphire, we focus on the epitaxial growth of LSMO only. A high resolution TEM image of the interface between LSMO and sapphire is shown in Fig. 2(c) with the major planes marked. The epitaxial relations between the film and the substrate after annealing, established through domain matching with six of $(1\bar{1}0)_{\text{LSMO}}$ planes matching with seven of $(2\bar{1}\bar{1}0)_{\text{Al}_2\text{O}_3}$ planes, are $(111)_{\text{LSMO}} // (0003)_{\text{Al}_2\text{O}_3}$ and $(1\bar{1}0)_{\text{LSMO}} // (2\bar{1}\bar{1}0)_{\text{Al}_2\text{O}_3}$. The lattice mismatch between $(1\bar{1}0)_{\text{LSMO}}$ and $(2\bar{1}\bar{1}0)_{\text{Al}_2\text{O}_3}$ is about 15.7%. We see that the interface has formed very regular domains of 1.6 nm size ($7 \times 0.236 \text{ nm}^2$).

Figure 3 shows the resistivity versus temperature, $\rho(T)$, of the as-grown and the postannealed films in an external magnetic field. The transport measurements were performed along the film surface using the four-probe method, and the magnetic field was applied normal to the film surface. The magnetoresistance (MR) (%) = $\{[\rho(H=0 \text{ T}) - \rho(H)] / \rho(H=0 \text{ T})\} \times 100$ was also depicted for the as-grown film. The $\rho(T)$ of the postannealed film is shown for $H=0 \text{ T}$ only since there was no practical difference at $H=1 \text{ T}$.

The resistivity of the as-grown film was two orders of magnitude larger than that of the postannealed film, with the latter having a similar resistivity as an epitaxial film.³ This

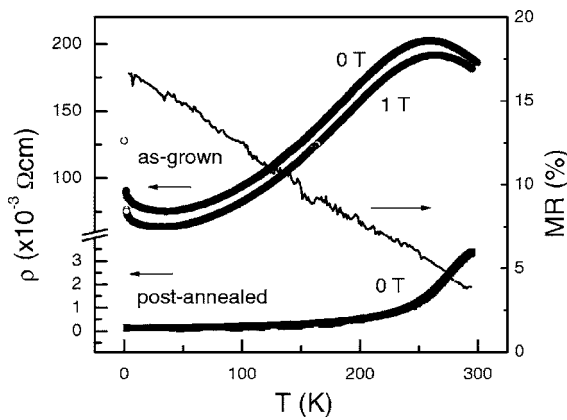


FIG. 3. Resistivity, $\rho(T)$, of the as-grown films (solid circles at $H=0$ T, open circles at $H=1$ T) and the postannealed films (solid square) at $H=0$ T as a function of temperature. The MR (solid line) of the as-grown films is also exhibited.

might be due to the additional grain boundaries and the presence of ZnO in the as-grown film. (Note that undoped ZnO has two to three orders higher resistivity than LSMO.) As higher values of resistivity in a granular or composite system have been reported in a number of studies,^{6–8} it is natural for our as-grown film with intermixed LSMO and ZnO to have higher resistivity than the postannealed film with clearly distinct and less resistive ZnAl_2O_4 grains.

In the as-grown film, a metal-insulator-transition-like feature was observed with a peak temperature (T_p) of around 260 K, which is considerably lower than the reported Curie temperature of LSMO ($T_C=330\text{--}365$ K).^{2,4,5} A large difference between T_p and T_C has previously been explained by grain boundary effects.¹⁴ According to the double exchange model, the metallicity occurs at the onset of ferromagnetism in single crystals and epitaxial thin films, causing T_p to coincide with T_C .¹⁴ However, in the polycrystalline or composite system, where the grain boundaries and/or insulating dopants play important roles in the transport phenomena, discrepancies between T_p and T_C are often observed.^{3,7}

As shown in Fig. 3, the MR of the as-grown film monotonously increased with the decrease of the temperature, reaching up to 16.5% at 10 K. Similar temperature dependence was previously observed in polycrystalline LSMO samples.³ The LFMR of the postannealed film was negligible ($\sim 1\%$) like those of epitaxial films.⁴

The resistivity ratio $\rho(H)/\rho(H=0$ T) of the as-grown film is shown in Fig. 4 as a function of the magnetic field at a temperature of 77 K. The maximum LFMR value of the film in an external magnetic field of 1 T was 12%. This is superior to that of epitaxial LSMO thin films² and is comparable to that of a $\text{La}_{0.7}\text{Sr}_{0.3}\text{MnO}_3:\text{Al}_2\text{O}_3$ composite film ($H=0.3$ T, 77 K)⁵ and many of the ceramic bulk composites.^{7,8}

The enhanced LFMR of our LSMO:ZnO composite thin films can also be interpreted by the mechanism of spin-polarized tunneling through magnetic tunnel junction structures. The large variation of resistance in granular manganites depending on the presence of a low external magnetic field has been ascribed both to high spin polarization and to the pinning of domain walls at grain boundaries. By incorporating ZnO, an artificial grain boundary effect could be obtained, maintaining the consistent orientation of LSMO

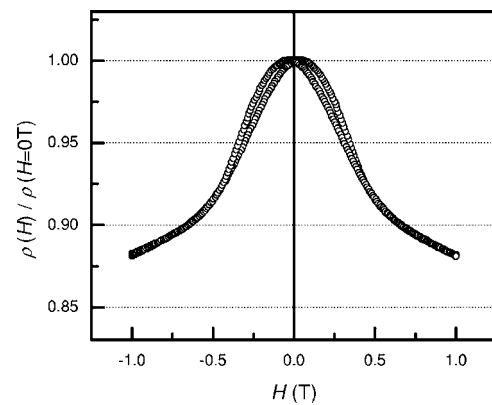


FIG. 4. Resistivity ratio $\rho(H)/\rho(H=0$ T) of the as-grown films as a function of magnetic field at a temperature of 77 K.

with respect to the sapphire substrate. Furthermore, the ZnO located at the interface of LSMO grains could build tunneling barriers to enhance spin-polarized tunneling.

In summary, we have deposited well-oriented $(\text{La}_{0.7}\text{Sr}_{0.3}\text{MnO}_3)_{0.5}:(\text{ZnO})_{0.5}$ nanocomposite thin films on single crystal sapphires via pulsed laser deposition. The as-grown films and the postannealed films have showed differences in their microstructures. An enhanced LFMR of $\sim 12\%$ has been achieved in the as-grown films with fine intermixed grains, while a negligible LFMR has been observed in the postannealed films with large single-crystal-like, clearly phase-separated grains.

This work was supported as a Los Alamos National Laboratory Directed Research and Development Project under the United States Department of Energy. The experiment at the NHMFL, Los Alamos was carried out under the auspices of the NSF, the State of Florida, and the US Department of Energy. The authors thank Dr. Yi Yuan for editing the manuscript.

¹S. Jin, T. H. Tiefel, M. McCormack, R. A. Fastnacht, R. Ramesh, and I. H. Chen, *Science* **264**, 413 (1994).

²Y. Suzuki, Y. Wu, J. Yu, U. Ruediger, A. D. Kent, T. K. Nath, and C. B. Eom, *J. Appl. Phys.* **87**, 6746 (2000).

³D. W. Kim, D. H. Kim, T. W. Noh, E. Oh, H. C. Kim, and H.-C. Lee, *Solid State Commun.* **121**, 631 (2002).

⁴E. S. Vlahov, K. Dorr, K.-H. Muller, K. A. Nenkov, A. Handstein, T. I. Donchev, A. Y. Spasov, and G. D. Beshkov, *Vacuum* **58**, 364 (2000).

⁵S. M. Liu, X. B. Zhu, J. Yang, B. C. Zhao, Z. G. Sheng, W. H. Song, J. M. Dai, and Y. P. Sun, *Physica B* **353**, 238 (2004).

⁶L. Yan, L. B. Kong, T. Yang, W. C. Goh, C. Y. Tan, C. K. Ong, M. A. Rahman, T. Osipowicz, and M. Q. Ren, *J. Appl. Phys.* **96**, 1568 (2004).

⁷D. K. Petrov, L. Krusin-Elbaum, J. Z. Sun, C. Field, and P. R. Duncombe, *Appl. Phys. Lett.* **75**, 995 (1999).

⁸L. Balcells, A. E. Carrillo, B. Martinez, and J. Fontcuberta, *Appl. Phys. Lett.* **74**, 4014 (1999).

⁹S. Gupta, R. Ranjit, C. Mitra, P. Raychaudhuri, and R. Pinto, *Appl. Phys. Lett.* **78**, 362 (2001).

¹⁰J.-M. Liu, G. L. Yuan, H. Sang, Z. C. Wu, X. Y. Chen, Z. G. Liu, Y. W. Du, Q. Huang, and C. K. Ong, *Appl. Phys. Lett.* **78**, 1110 (2001).

¹¹V. Moshnyaga, B. Damaschke, O. Shapoval, A. Belenchuk, J. Faupel, O. I. Lebedev, J. Verbeeck, G. Van Tendeloo, M. Mucksch, V. Tsurkan, R. Tidecks, and K. Samwer, *Nat. Mater.* **2**, 247 (2003).

¹²L. Meda, C. Bacaltchuk, H. Garmestani, and K.-H. Dahmen, *J. Mater. Sci.: Mater. Electron.* **12**, 143 (2001).

¹³K.-K. Choi, T. Taniyama, and Y. Yamazaki, *J. Appl. Phys.* **90**, 6145 (2001).

¹⁴J. Y. Gu, C. Kwon, M. C. Robson, Z. Trajanovic, K. Ghosh, R. P. Sharma, R. Shreekala, M. Rajeswari, T. Venkatesan, R. Ramesh, and T. W. Noh, *Appl. Phys. Lett.* **70**, 1763 (1997).